

Experimental Analysis of Communication Relaying Delay in Low-Energy Ad-hoc Networks

Taichi Miya*, Kohta Ohshima†, Yoshiaki Kitaguchi* and Katsunori Yamaoka*

*Tokyo Institute of Technology, Ookayama 2-12-1-S3-68, Meguro-ku, Tokyo, 152-8552 Japan

E-mail: miya@net.ict.e.titech.ac.jp, kitaguchi@gsic.titech.ac.jp, yamaoka@ict.e.titech.ac.jp

†Tokyo University of Marine Science and Technology, Etchujima 2-1-6, Koto-ku, 135-8533 Japan

E-mail: kxoh@kaiyodai.ac.jp

Abstract—In recent years, more and more applications use ad-hoc networks for local M2M communications, but in some cases such as when using WSNs, the software processing delay induced by packets relaying may not be negligible. In this paper, we planned and carried out a delay measurement experiment using Raspberry Pi Zero W. The results demonstrated that, in low-energy ad-hoc networks, processing delay of the application is always too large to ignore; it is at least ten times greater than the kernel routing and corresponds to 30% of the transmission delay. Furthermore, if the task is CPU-intensive, such as packet encryption, the processing delay can be greater than the transmission delay and its behavior is represented by a simple linear model. Our findings indicate that the key factor for achieving QoS in ad-hoc networks is an appropriate node-to-node load balancing that takes into account the CPU performance and the amount of traffic passing through each node.

Index Terms—Ad-hoc network, processing delay, measurement experiment, Raspberry Pi Zero W

I. INTRODUCTION AND RELATED WORKS

An ad-hoc network is a self-organizing network that operates independently of pre-existing infrastructures such as wired backbone networks or wireless base stations by having each node inside the network behave as a repeater. It is a kind of temporary network that is not intended for long-term operation. Every node of an ad-hoc network needs to be tolerant of dynamic topology changes and have the ability to organize the network autonomously and cooperatively.

Because of these specific characteristics, since the 1990s, ad-hoc networks have played an important role as a mean for instant communication in environments where the network infrastructure is weak or does not exist, such as developing countries, disaster areas, and battle fields. However, in recent years, the ad-hoc network is also a hot topic in urban areas where the broadband mobile communication systems are well developed and always available. More and more applications use ad-hoc networks for local M2M communications, especially in key technologies that are expected to play a vital role in future society, such as intelligent transportation systems (ITS) supporting autonomous car driving, cyber-physical systems (CPS) like smart grids, wireless sensor networks (WSN), and applications like the IoT platform.

These days, communication entities are shifting from humans to things; the network infrastructures tend to require a more strict delay guarantee, and the ad-hoc network is no

exception. There have been many prior studies about delay-aware communication in the field of ad-hoc networks [1]–[4]. Most of these focus on the link delay and only a few consider both node and link delays [1], [2]. However, in some situations where the power consumption is severely limited (e.g., with WSN), the communication relaying cost of small devices with low-power processors may not be negligible for the end-to-end delay of each communication.

It is necessary to discuss, on the basis of actual data measured on wireless ad-hoc networks, how much the link and node delays account for the end-to-end delay. In the field of wired networks, there have been many studies reporting measurement experiments of packet processing delay as well as various proposals for performance improvement [5]–[10]. In addition, the best practice of QoS measurement has been discussed in the IETF [11]. In the past, measurement experiments on ASIC routers have been carried out for the purpose of benchmarking routers working on ISP backbones [5]–[7]; in contrast, since the software router has emerged as a hot topic in the last few years, recent studies mainly concentrate on the bottleneck analysis of the Linux kernel’s network stack [8]–[10]. There has also been a study focusing on the processing delay caused by the low-power processor assuming interconnection among small robots [12]. However, as far as we know, no similar measurement exists in the field of wireless ad-hoc networks. Therefore, many processing delay models have been considered so far, e.g., simple linear approximation [13] or queueing model-based nonlinear approximation [14], but it is hard to determine which one is the most reasonable for wireless ad-hoc networks.

In this work, we analyze the communication delay in an ad-hoc network through a practical experiment using Raspberry Pi Zero W. We assume an energy-limited ad-hoc network composed of small devices with low-power processors. Our goal is to support the design of QoS algorithms on ad-hoc networks by clarifying the impact of software packet processing on the end-to-end delay and presenting a general delay model to which the measured delay can be adapted. This is an essential task for future ad-hoc networks and their related technologies.

First, we briefly describe the structure of the Linux kernel network stack in Sect. II. We explain the details of our measurement experiment in Sects. III and IV, and report

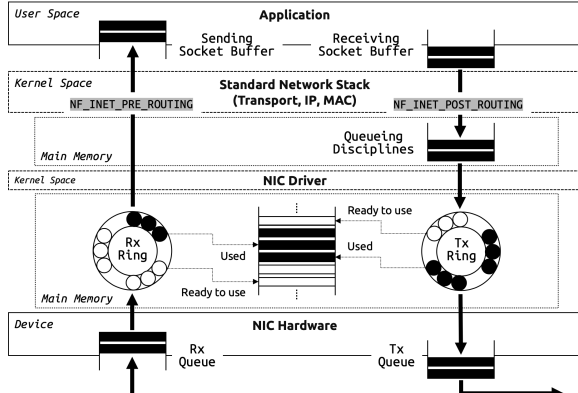


Fig. 1: Packet queueing in the Linux network stack.

the results in Sect. V. We conclude in Sect. VI with a brief summary and mention of future work.

II. NETWORK STACK OF LINUX KERNEL

In this section, we present a brief description of the Linux kernel's standard network stack from the viewpoints of the packet receiving and sending sequences.

A. Generic Packet Receiving Sequence

Figure 1 shows the flow of packets in the network stack from the perspective of packet queueing.

First, as the preparation for receiving packets, the NIC driver allocates memory resources in RAM that can store a few packets, and has packet descriptors (Rx descriptors) hold these addresses. The Rx ring buffer is a descriptor ring located in RAM, and the driver notifies the NIC of the head and tail addresses of the ring. The NIC then fetches some unused descriptors by direct memory access (DMA) and waits for the packets to arrive. The workflow after the packet arrival is as follows. As a side note, the below sequence is a receiving mechanism called new API (NAPI) supported in Linux kernel 2.6 or later.

- i) Once a packet arrives, NIC writes the packet out as an `sk_buff` structure to RAM with DMA, referring to the Rx descriptors cached beforehand, and issues a HardIRQ after the completion.
- ii) The IRQ handler receiving HardIRQ pushes it by `napi_schedule()` to the `poll_list` of a specific CPU core and then issues SoftIRQ so as to get the CPU out of the interrupt context.
- iii) The soft IRQ scheduler receiving SoftIRQ calls the interrupt handler `net_rx_action()` at the best timing.
- iv) `net_rx_action()` calls `poll()`, which is implemented in not the kernel but the driver, for each `poll_list`.
- v) `poll()` fetches `sk_buff` referring to the ring indirectly and pushes it to the application on the upper layer. At this time, packet data is transferred from RAM to RAM; that is, the data is copied from the memory in the kernel space to the receiving socket buffer in the user space by

`memcpy()`. Repeat this memory copy until the `poll_list` becomes empty.

- vi) The application takes the payload from the socket buffer by calling `recv()`. This operation is asynchronous with the above workflows in the kernel space. The packet receiving sequence is completed when all the payloads have been retrieved.

B. Generic Packet Sending Sequence

In the packet sending sequence, all the packets basically follow the reverse path of the receiving sequence, but they are stored in a buffer called QDisc before being written to the Tx ring buffer (Fig. 1).

The ring buffer is a simple FIFO queue that treats all arriving packets equally. This design simplifies the implementation of the NIC driver and allows it to process packets fast. QDisc corresponds to the abstraction of the traffic queue in the Linux kernel and makes it possible to achieve a more complicated queueing strategy than FIFO without modifying the existing codes of the kernel network stack or drivers.

QDisc supports many queueing strategies; by default, it runs in `pfifo_fast` mode. If the packet addition fails due to a lack of free space in QDisc, the packet is pushed back to the upper layer socket buffer.

III. EXPERIMENTAL DESIGN

As discussed in Sect. I, the goal of this study is to evaluate the impact of software packet processing, induced by packet relaying, to the end-to-end delay, on the basis of an actual measurement assuming an ad-hoc network consisting of small devices with low-power processors. Figure 2 shows our experimental environment, whose details are described in Sect. IV.

A. Definitions of Delays in Network

We define the classification of communication delays as below. Both *processing delay* and *queueing delay* correspond to the application delay in a broad sense.

- **End-to-end delay:** Total of node delays and link delays
- **Node delay:** Sum of *processing delay*, *queueing delays*, and any processing delays occurring in the network stack
- **Link delay:** Sum of all other delays occurring under the NIC driver, such as queueing delay of the NIC internal buffer, transmission delay and propagation delay at the communication medium
- **Processing delay:** Processing delay for packet relaying generated by the application in user space
- **Queueing delay:** Queueing delay at the socket buffer

B. Proxy: How to Relay Packets

The proxy node (Fig. 2) relays packets with the three methods below, and we evaluate the effect of each in terms of the end-to-end delay. By comparing the results of *OLSR* and *AT*, we can clarify the delay caused by packets passing through the network stack.

- **Kernel routing (OLSR):** Proxy relays packets by kernel routing based on the OLSR routing table. In this case, the



Fig. 2: Three Raspberry Pis connected logically inline.

relaying process is completed in kernel space because all packets are wrapped in L3 of the network stack. Accordingly, both *processing delay* and *queueing delay* defined above become zero, and node delay is purely equal to the processing delay on the network stack in the kernel space.

- **Address translation (AT):** Proxy works as a TCP/UDP proxy, and all packets are raised to the application running in the user space. The application simply relays packets by switching sockets, which is equivalent to a fixed-length header translation.
- **Encryption (Enc):** Proxy works as a TCP/UDP proxy. Besides AT, the application also encrypts payloads using AES 128-bit in CTR mode so that the relaying load depends on the payload size.

C. Measurement Conditions

For each relaying method, we conduct measurements with variations of the following conditions. We express all the results as multiple percentile values in order to remove delay spikes. Because the experiment takes several days, we record the RSSI of the ad-hoc network including five surrounding channels.

- **Payload size**
- **Packets per second (pps)**
- **Additional CPU load (stress)**

IV. MEASUREMENT METHODS

In this section, we explain the technical details of the experimental environment and measurement programs.

A. Building OLSR Ad-hoc Network

We use three Raspberry Pi Zero Ws (see Table I for the hardware specs). The Linux distributions installed on the Raspberry Pis are Raspbian and the kernel version is 4.19.97+.

We use OLSR (RFC3626), which is a proactive routing protocol, and adopt `olsrd` as its actual implementation. Since all three of the nodes are location fixed, even if we used a reactive routing protocol like AODV instead of OLSR, only the periodic Hello in OLSR will change the periodic RREQ induced by the route cache expiring; that is, in this experiment, whether the protocol is proactive or reactive does not have a significant impact on the final results.

The ad-hoc network uses channel 9 (2.452 GHz) of IEEE 802.11n, transmission power is fixed to -31 dBm, and bandwidth is 20 MHz. As WPA (TKIP) and WPA2 (CCMP) do not support ad-hoc mode, the network is not encrypted.

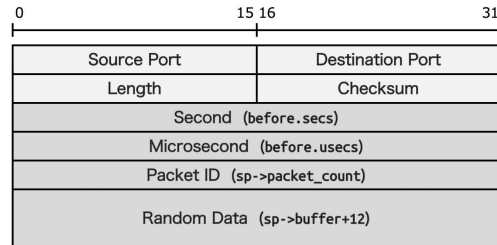


Fig. 3: Format of UDP probe generated by iperf.

Although the three nodes can configure an OLSR mesh, as they are located physically close to each other, we have the sender/receiver drop OLSR Hello from the receiver/sender as well as the ARP response by Netfilter so that the network topology becomes a logically inline single-hop network, as shown in Fig. 2.

B. Preparation of Traffic Generator

We use `iperf` as a traffic generator and measure the UDP performance as it transmits packets from sender to receiver via proxy. The `iperf` embeds two timestamps and a packet ID in the first 12 bytes of the UDP data section (Fig. 3), and the following measurement programs we implement use this ID to identify each packet. Random data are generated when `iperf` starts getting entropy from `/dev/urandom`, and the same series is embedded in all packets.

C. Implementation of the Kernel Module for Measurement

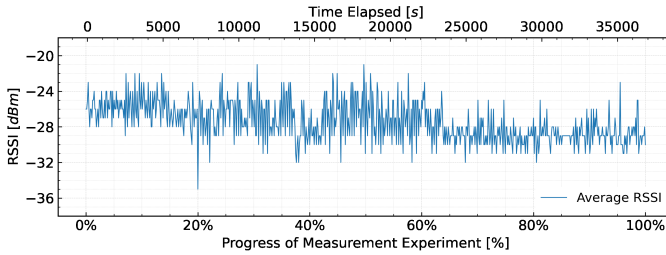
We create a loadable kernel module using Netfilter and measure the *queueing delay* in receiving and sending UDP socket buffers. The workflow is summarized as follows: the module hooks up the received packets with `NF_INET_PRE_ROUTING` and the sent packets with `NF_INET_POST_ROUTING` (Fig. 1), retrieves the packet IDs `iperf` marked by indirectly referencing the `sk_buff` structure, and then writes them out to the kernel ring buffer via `printk()` with a timestamp obtained by `ktimer_get()`.

D. Implementation of the Proxy

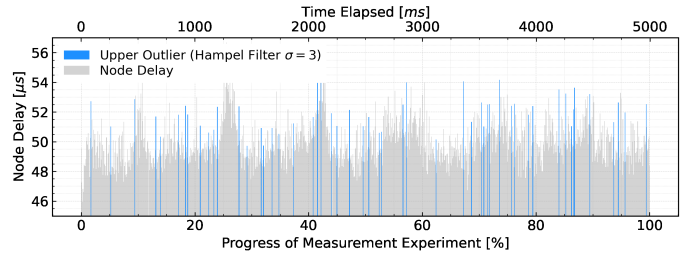
The proxy program is the application running in the user space. It creates `AF_INET` sockets between sender and proxy as well as between proxy and receiver and then translates IP addresses and port numbers by switching sockets. Furthermore, it records the timestamps obtained by `clock_gettime()` immediately after calling `recv()` and `sendto()`, and encrypts every payload data protecting the first 12 bytes of metadata marked by `iperf` so as not to be rewritten. The above refers to the UDP proxy; the TCP proxy we prepare simply using `socat`.

TABLE I: Hardware specs of Raspberry Pi Zero W.

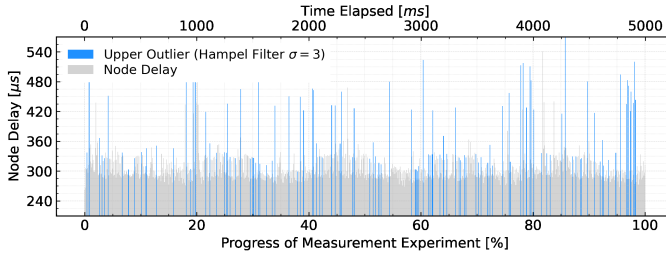
SoC	Broadcom BCM2835
CPU	ARM1176JZF-S (ARMv6) 1core 1GHz
RAM	LPDDR2 SDRAM 512MB
Wi-Fi	IEEE 802.11b,g,n 2.4GHz
Power	150mA (0.75W)
Size	65mm x 30mm (9g)



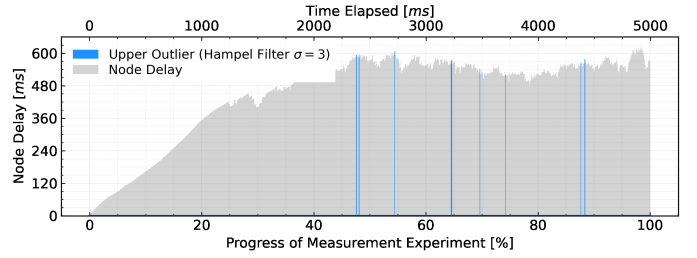
(a) **RSSI**: Average scores for sender, proxy, and receiver.



(b) **Node delay (OLSR)**: 1000 bytes, 200 pps, 0% stress



(c) **Node delay (AT)**: 1000 bytes, 200 pps, 0% stress



(d) **Node delay (Enc)**: 1000 bytes, 200 pps, 0% stress

Fig. 4: **Timelines**: Average time variation of RSSI and 100th percentile node delays during the measurement.

E. Additional CPU Load at Proxy

We execute a dummy process whose CPU utilization rate is limited by `cpulimit` as a controlled noise of the user space in order to investigate and clarify its impact on the node delay.

V. RESULTS AND DISCUSSION

We performed the delay measurement experiments under the conditions shown in Table II using the methods described in the previous section. Due to the space constraints, we omit the results of the preliminary experiment. Note that all experiments were carried out at the author's home; due to the Japanese government's declaration of the COVID-19 State of Emergency, we have had to stick to the "Stay home" initiative unless absolutely necessary.

A. Time Variation of Received Signal Strength Indicator

The experiment was divided into nine measurements. Figure 4a shows the time variation of RSSI during a measurement. We were unable to obtain SNRs owing to the specifications of the Wi-Fi driver, and thus the noise floors were unknown, but the ESSIDs observed in the five surrounding channels were all less than -80 dBm. The RSSI variabilities were also within the range that did not affect the modulation and coding scheme (MCS) [15]; therefore, it appears that the link quality was sufficiently high throughout all measurements.

B. Time Variation of Node Delay and Coffee-break Effect

Figures 4b, 4c, and 4d shows the average time variations of node delay, which were the results under the condition of 1000 bytes, 200 pps, and 0% *stress*. The blue highlighted bars indicate upper outliers (delay spikes) detected with a Hampel filter ($\sigma = 3$). There were 53 outliers in *OLSR*, 115 in *AT*, and 9 in *Enc*.

In general, when the CPU receives periodic interrupts (e.g., routing updates, SNMP requests, GCs of RAM), packet forwarding is paused temporarily so that the periodic delay spikes can be observed in the end-to-end delay. This phenomenon is called the "coffee-break effect" [7] and has been mentioned in several references [5], [8], [9].

For this experiment, as seen in the results of *AT* (Fig. 4c), in the low-energy ad-hoc networks, it is evident that the CPU-robbing by other processes like coffee-break had a significant impact on the communication delay. Incidentally, there were fewer spikes under both 1) *OLSR* and 2) *Enc* than under *AT*. 1) Since the packet forwarding was completed within the kernel space, node delay was less susceptible to applications running in the user space. 2) Since the payload encryption was overwhelmingly CPU-intensive, the influence of other applications was hidden and difficult to observe from the node delay.

C. Jitter and Packet Loss Rate

Figures 5a and 5b shows the jitter of one-way communication delay. Lines represent the average values, and we filled in the areas between the minimum and the maximum. There were no significant differences between *OLSR* and *AT*, which suggests that lifting packets to the application layer does not affect jitter. Jitter increased in proportion to the payload size only in the case of *Enc*.

TABLE II: Parameter settings for measurement experiments.

Payload size	100, 200, 300, ..., 1400 [bytes]
packets per second	200, 400, 600, ..., 1200 [pps]
packets per second (<i>Enc</i>)	20, 40, 60, ..., 400 [pps]
Additional CPU load (<i>stress</i>)	0, 50, 90 [%]
Transmission duration	5 [sec]
Number of samples	50

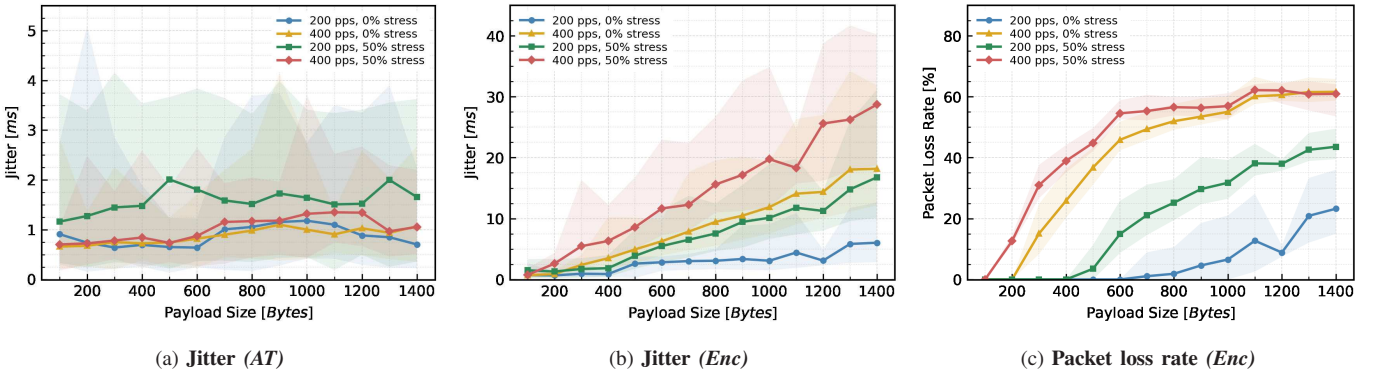


Fig. 5: **Jitter and packet loss rates:** 100th percentile values under several conditions.

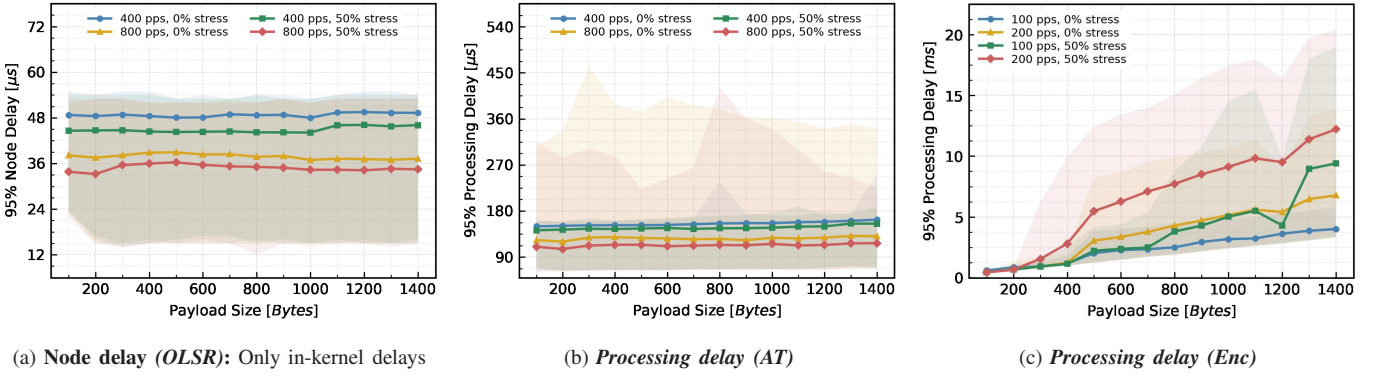


Fig. 6: **Node and processing delays:** 95th percentile delays under the several conditions.

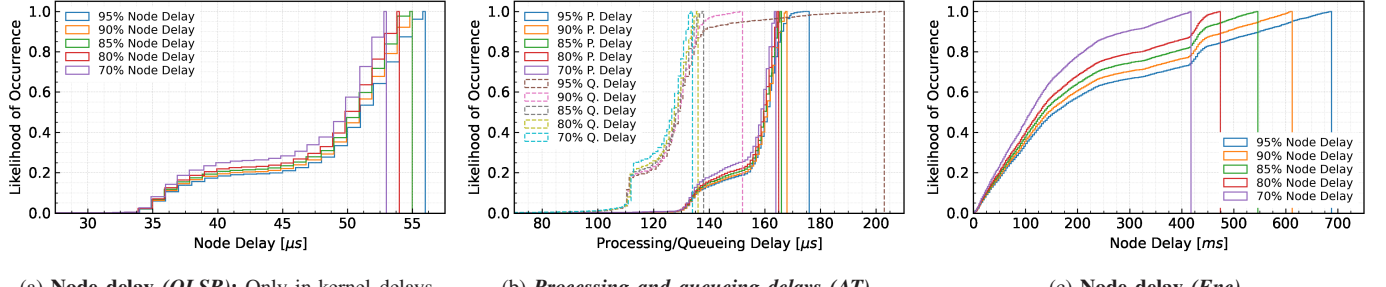


Fig. 7: **Empirical Cumulative Distribution Function:** Several percentile node delays under 1000 bytes, 200 pps and 0% stress.

Similarly, only in the case of *Enc* with 200 pps or more, the packet loss rate tended to increase with payload size, drawing a logarithmic curve as seen in Fig. 5c; in all other cases, no packet loss occurred regardless of the conditions.

D. Node Delay

Figure 6 shows the tendency of the node delay variation against several conditions, and Fig. 7 shows the likelihood of occurrence as empirical CDF.

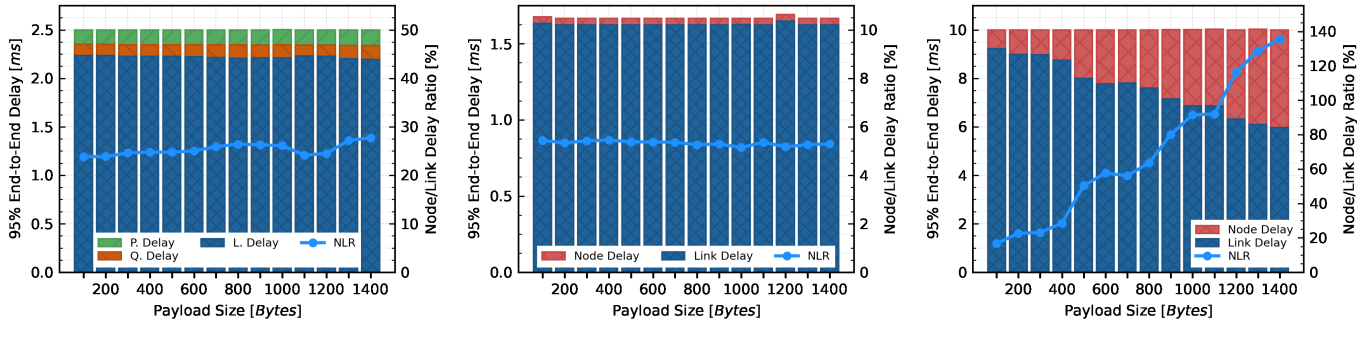
According to these figures, in the cases of *OLSR* and *AT*, the delay was nearly constant irrespective of pps and *stress*. There was a correlation between the variation and pps in *OLSR*, while in *AT* there was not; this suggests that the application-level packet forwarding is less stable than kernel routing from the perspective of node delay. In the case of *Enc*, the *processing delay* increased to the millisecond order and

increased approximately linearly with respect to the payload size, and the delay variance became large overall. In addition, the graph tended to be smoothed as the pps increased; this arises from the fact that packet encryption takes up more CPU time, which makes the influence of other processes less conspicuous.

It appears that the higher the pps, the lower the average delay (Fig. 6a and 6b), and the delay variance decreases around 1200 bytes (Fig. 6c), but the causes of these remain unknown, and further investigation is required. One thing is certain: on the Raspberry Pi, pulling the packets up to the application through the network stack results in a delay of more than 100 microseconds.

E. Link Delay vs. Node Delay

Figure 8 shows the breakdown of the end-to-end delay and also describes the node delay link delay ratio (NLR). As we



(a) **E2E delay (OLSR):** 400 pps, 0% stress

(b) **E2E delay (AT):** 400 pps, 0% stress

(c) **E2E delay (Enc):** 100 pps, 0% stress

Fig. 8: **End-to-end delay:** 95th percentile end-to-end delays including node and link delays.

saw in Fig. 2, for this experimental environment, the end-to-end delay included two link delays, and the link delay shown in Fig. 8 is the sum of them. The link delay was calculated from the effective throughput reported in iperf. As iperf does not support pps as its option, we achieved it by adjusting the amount of transmitted traffic, as

$$\text{bandwidth} = \text{pps} \times \text{size} \times 8. \quad (1)$$

The results showed that, in the cases of *OLSR* and *AT*, the NLR was almost constant with respect to the payload size, while in *Enc*, it showed an approximately linear increase. The NLR was less than 5% in *OLSR*, while in *AT*, it was around 30%, which cannot be considered negligible. Furthermore, node delay was greater than link delay when the payload size was over 1200 bytes in *Enc*.

VI. CONCLUSION AND FUTURE WORK

In this work, we have designed and conducted an experiment to measure the software processing delay caused by packets relaying. The experimental environment is based on an *OLSR* ad-hoc network composed of Raspberry Pi Zero Ws. The results were qualitatively explainable, and suggested that, in low-energy ad-hoc networks, there are some situations where the processing delay cannot be ignored.

- The relaying delay of kernel routing is usually negligible, but when it is handled by application, the delay can be more than ten times greater, however simple the task is.
- If an application performs CPU-intensive tasks such as encryption or full translation of protocol stacks, the delay increases according to the linear model and can be greater than the link's transmission delay.

For this reason, node-to-node load balancing considering the CPU performance or amount of passing traffic could be extremely useful for achieving delay-guaranteed routing in ad-hoc networks. Particularly in heterogeneous ad-hoc networks (HANETs), where each node's hardware specs are different from each other, the accuracy of passing node selection would have a significant impact on the end-to-end delay.

As we did not take any noise countermeasures in this experiment, our future work will involve similar measurements in an anechoic chamber to reduce the noise from external waves and an investigation of the differences in results.

REFERENCES

- [1] T. Miya, K. Ohshima, Y. Kitaguchi, and K. Yamaoka, "The upper limit of flow accommodation under allowable delay constraint in hanets," in *2019 16th IEEE Annual Consumer Communications & Networking Conference (CCNC)*. IEEE, 2019, pp. 1–2.
- [2] Y. Miao, S. Vural, Z. Sun, and N. Wang, "A unified solution for gateway and in-network traffic load balancing in multi-hop data collection scenarios," *IEEE Systems Journal*, vol. 10, no. 3, pp. 1251–1262, 2015.
- [3] L. Chen and W. B. Heinzelman, "Qos-aware routing based on bandwidth estimation for mobile ad hoc networks," *IEEE Journal on selected areas in communications*, vol. 23, no. 3, pp. 561–572, 2005.
- [4] M. A. Gawas, K. Modi, P. Hurkat, and L. J. Gudino, "Qos based multipath routing in manet: A cross layer approach," in *2017 International Conference on Communication and Signal Processing (ICCP)*. IEEE, 2017, pp. 1806–1812.
- [5] K. Papagiannaki, S. Moon, C. Fraleigh, P. Thiran, and C. Diot, "Measurement and analysis of single-hop delay on an ip backbone network," *IEEE Journal on Selected Areas in Communications*, vol. 21, no. 6, pp. 908–921, 2003.
- [6] C. Lee, C. Park, K. Jang, S. Moon, and D. Han, "Dx: Latencybased congestion control for datacenters," *IEEE/ACM Transactions on Networking*, vol. 25, no. 1, pp. 335–348, 2016.
- [7] D. Sanghi, A. K. Agrawala, O. Gudmundsson, and B. N. Jain, "Experimental assessment of end-to-end behavior on internet," in *IEEE INFOCOM'93 The Conference on Computer Communications, Proceedings*. IEEE, 1993, pp. 867–874.
- [8] L. Angrisani, G. Ventre, L. Peluso, and A. Tedesco, "Measurement of processing and queuing delays introduced by an open-source router in a single-hop network," *IEEE transactions on instrumentation and measurement*, vol. 55, no. 4, pp. 1065–1076, 2006.
- [9] A. Beifuß, D. Raumer, P. Emmerich, T. M. Runge, F. Wohlfart, B. E. Wolfinger, and G. Carle, "A study of networking software induced latency," in *2015 International Conference and Workshops on Networked Systems (NetSys)*. IEEE, 2015, pp. 1–8.
- [10] K. M. Salehin, R. Rojas-Cessa, C.-b. Lin, Z. Dong, and T. Kijkanjanarat, "Scheme to measure packet processing time of a remote host through estimation of end-link capacity," *IEEE Transactions on Computers*, vol. 64, no. 1, pp. 205–218, 2013.
- [11] G. Almes, S. Kalidindi, M. J. Zekauskas, and A. Morton, "A One-Way Delay Metric for IP Performance Metrics (IPPM)," RFC 7679, Jan. 2016. [Online]. Available: <https://rfc-editor.org/rfc/rfc7679.txt>
- [12] C. S. V. Gutiérrez, L. U. S. Juan, I. Z. Ugarte, and V. M. Vilches, "Real-time linux communications: an evaluation of the linux communication stack for real-time robotic applications," *arXiv preprint arXiv:1808.10821*, 2018.
- [13] R. Ramaswamy, N. Weng, and T. Wolf, "Characterizing network processing delay," in *IEEE Global Telecommunications Conference*, 2004. GLOBECOM'04., vol. 3. IEEE, 2004, pp. 1629–1634.
- [14] S. Yashkov, "Processor-sharing queues: Some progress in analysis," *Queueing systems*, vol. 2, no. 1, pp. 1–17, 1987.
- [15] Y. Daldoul, D.-E. Meddour, and A. Ksentini, "Ieee 802.11 n/ac data rates under power constraints," in *2018 IEEE International Conference on Communications (ICC)*. IEEE, 2018, pp. 1–6.